CROSS–VALIDATION OF NUMERICAL SCHEMES FOR EXTENDED HYDRODYNAMICAL MODELS OF SEMICONDUCTORS

ANGELO MARCELLO ANILE

Dipartimento di Matematica, Università di Catania
viale A. Doria 6 - 95125 Catania, Italy

MICHAEL JUNK

Fachbereich Mathematik, Universität Kaiserslautern
Postfach 3049, 67653 Kaiserslautern, Germany

VITTORIO ROMANO

Politecnico di Bari, sede di Taranto
Viale del Turismo 8 - 74100 Taranto, Italy

GIOVANNI RUSSO

Dipartimento di Matematica, Università dell'Aquila
Via Vetoio, loc. Coppito - 67100 L'Aquila

The numerical integration of the hydrodynamical model of semiconductors based on Extended Thermodynamics has been tackled. On account of the mathematical complexity of the system no theoretical conditions of convergence are available for the existing schemes. Therefore in order to lend confidence to the obtained numerical solution it was almost mandatory to resort to a cross-validation comparing the results given by two different methods. The Kinetic Scheme and the finite difference method represented by a suitable modification of the Nessyahu-Tadmor scheme furnish numerical results for the ballistic diode problem in good agreement even for non smooth solutions.

1. Introduction

In the past, moment methods for solving transport equations[23] have been somehow overshadowed by more direct particle methods because they are plagued with some difficulties and ambiguities, essentially related to the closure problem (and also to the correct limiting behavior near local thermal equilibrium). However, moment methods have retained some appeal because they lead to a nice mathematical structure (PDE's for variables which, at least for the lower moments, present a clear physical interpretation). Furthermore they lead to results which are free from the inherent noisiness of the particle methods and are computationally much less expensive. Lately, moment methods have been revisited by Levermore[19] who set the

1

closure problem in a well defined mathematical context finding a rational solution to it with the maximum entropy ansatz. Furthermore Levermore also gives recipes for alleviating the problem of the correct limiting behavior near thermal equilibrium (a problem connected with the truncation of the collision operator).

In the physics literature a similar approach has already been introduced[16,24] and lends itself to an intriguing physical interpretation which is called extended thermodynamics. It is an extension of ordinary thermodynamics to cope with far from equilibrium situations. Recently, the methods of extended thermodynamics and maximum entropy closure have been applied to the modeling of charged carrier transport in semiconductors[1,2,4,5] and lead to an extended hydrodynamical model which shows satisfactory agreement with Monte Carlo simulations. The resulting mathematical model consists of a set of PDE expressing balance laws for particle number, momentum, energy and energy flux, coupled with the Poisson equation.

In the semiconductor applications one encounters density gradients which are substantially larger than those usual in hydrodynamics. Therefore the numerical solution for the hyperbolic part of the model (the balance laws) requires a rather accurate method capable of dealing with discontinuities. Because of the extreme variations which are encountered in the numerical solution it is mandatory to apply different algorithms in order to be confident of the obtained results. Besides the well known scheme by Nessyahu and Tadmor [26] which is easily applicable to our system because it does not require the knowledge of the characteristic structure (which is typically difficult for higher dimensional systems) we have resorted also to Kinetic Schemes which are based on a completely different philosophy.[9,18,28] As we shall see, the fact that the two rather different methods lead to the same results for non trivial cases, lends confidence to the obtained numerical solution.

One reason for adopting Kinetic Schemes is that, since they arise from the kinetic origin of the system of PDE's, they are natural candidates to be used for hybrid models (those in which in some regions of the domain a reduced moment system is adopted, whereas in other regions, a fully kinetic description is mandatory). Another reason is that, by using Kinetic Schemes, it is possible to incorporate positivity properties and boundary conditions (such as incoming and outgoing fluxes) which are not easily enforced with other methods.

The outline of the paper is as follows. In Sections 2 and 3 the mathematical model is presented and the domain of hyperbolicity is analyzed. In Section 4 we describe the Kinetic Schemes while in Section 5 the finite difference method is presented. This latter is constituted by the Nessyahu-Tadmor scheme for hyperbolic systems with suitable modification in order to include also the presence of a source term in the evolution equations. In the last section we discuss the results of the numerical simulation of a silicon ballistic $n^+ - n - n^+$ diode.

2. Mathematical Model

In a semi classical approximation,[23] a kinetic description of electrons in a semiconductor is given by a transport equation for the one particle distribution function

$f(\boldsymbol{x}, \boldsymbol{k}, t)$, which represents the probability of finding an electron at time t in an elementary volume $d\boldsymbol{x}d\boldsymbol{k}$, around position $\boldsymbol{x}$ and with crystal momentum $\boldsymbol{k}$,

$$\frac{\partial f}{\partial t} + v_i(\boldsymbol{k})\frac{\partial f}{\partial x_i} - \frac{e}{\hbar}E_i\frac{\partial f}{\partial k_i} = \mathcal{C}[f]. \tag{2.1}$$

Here e is (the absolute value of) the electron charge, and $\boldsymbol{k}$ represents the crystal momentum of the electron, belonging to the first Brillouin zone.* $\boldsymbol{E}$ is the electric field, and is related to the electron distribution by Poisson's equation:

$$E_i = \frac{\partial \phi}{\partial x_i},$$
$$\epsilon \Delta \phi = -e(N_D - N_A - n),$$

where ϕ is the electric potential, ϵ is the permittivity of the semiconductor, N_D and N_A are respectively the donor and acceptor density, and n is the electron density. The latter is related to f by

$$n = \int f d\boldsymbol{k}.$$

$\mathcal{C}[f]$ is the collision term, which takes into account scattering with acoustical and optical phonons and with impurities. Its expression is of the form:

$$\mathcal{C}[f] = \int d\boldsymbol{k}' \left[s(\boldsymbol{x}, \boldsymbol{k}', \boldsymbol{k})f'(1 - f) - s(\boldsymbol{x}, \boldsymbol{k}, \boldsymbol{k}')f(1 - f') \right]. \tag{2.2}$$

The first term gives the total probability that an electron at $\boldsymbol{x}$ with momentum $\boldsymbol{k}'$ is scattered to the state $(\boldsymbol{x}, \boldsymbol{k})$, while the second term gives the total probability that an electron in $(\boldsymbol{x}, \boldsymbol{k})$ is scattered to $(\boldsymbol{x}, \boldsymbol{k}')$.

The electron velocity $\boldsymbol{v}(\boldsymbol{k})$ depends on the energy $\mathcal{E}$ measured from the conduction band minimum by the relation

$$\boldsymbol{v}(\boldsymbol{k}) = \nabla_{\boldsymbol{k}}\mathcal{E}.$$

In general the band structure may be very complicated, and it depends on the material. In the approximation of a single parabolic band (which we adopt in the rest of the paper), the effective mass is a constant scalar m^*, and the relation between energy and wave vector is

$$\mathcal{E} = \frac{\hbar^2|\boldsymbol{k}|^2}{2m^*},$$

and therefore

$$v_i = \frac{\hbar}{m^*}k_i.$$

---

*Einstein summation over repeated indices is used, and physical units are such that $\hbar = 1$.

Consistently the first Brillouin zone is extended to $\mathbb{R}^3$. Besides the electron density n, other physically relevant moments are the momentum $\boldsymbol{J}$ and the closely related average velocity $\boldsymbol{u}$ (relative to the crystal, assumed to be at rest)

$$\boldsymbol{J} = n\boldsymbol{u} = \int_{\mathbb{R}^3} \boldsymbol{v}(\boldsymbol{k}) f \, d\boldsymbol{k}.$$

The total energy W, which is the sum of kinetic energy and internal energy is related to the second order moment

$$W = \frac{m^*}{2} n |\boldsymbol{u}|^2 + \frac{3}{2} n k_B T = \int_{\mathbb{R}^3} \frac{m^*}{2} |\boldsymbol{v}(\boldsymbol{k})|^2 f \, d\boldsymbol{k}.$$

T is the temperature of the electron gas and $p = n k_B T$ its pressure. These quantities can also be expressed as moments of f if we go over to the peculiar velocity $c(\boldsymbol{k}) = v(\boldsymbol{k}) - \boldsymbol{u}$. Then

$$\frac{3}{2} n k_B T = \frac{3}{2} p = \int_{\mathbb{R}^3} \frac{m^*}{2} |\boldsymbol{c}(\boldsymbol{k})|^2 f \, d\boldsymbol{k}.$$

The physical interpretation of the third order moment

$$\boldsymbol{S} = \int_{\mathbb{R}^3} \frac{m^*}{2} |\boldsymbol{v}(\boldsymbol{k})|^2 \boldsymbol{v}(\boldsymbol{k}) f \, d\boldsymbol{k}$$

is energy flux and accordingly

$$\boldsymbol{q} = \int_{\mathbb{R}^3} \frac{m^*}{2} |\boldsymbol{c}(\boldsymbol{k})|^2 \boldsymbol{c}(\boldsymbol{k}) f \, d\boldsymbol{k}$$

is the heat flux. The second order moments corresponding to the anisotropic stress tensor

$$\sigma_{ij} = \int_{\mathbb{R}^3} m^* \left(c_i c_j - \frac{1}{3} |\boldsymbol{c}|^2 \delta_{ij} \right) f \, d\boldsymbol{k}$$

will play only a subordinate role in this article because we later assume $\sigma_{ij} = 0$ to derive a reduced model.

Equation (2.1) is a nonlinear integro-differential equation in seven independent variables. Simpler approximate models can be derived from the kinetic equation. The main approximations are based on the expansion of the distribution function around the Maxwell-Boltzmann equilibrium distribution (e.g. Drift-Diffusion model), and the moment method (hydrodynamical models).

Hydrodynamical models are obtained from the infinite hierarchy of moment equations corresponding to (2.1) by assuming an appropriate expression for the (N+1)–order moment in terms of the previous ones. Apart from this closure problem the modeling of the production terms is also necessary. The closure assumptions which we adopt is the maximum entropy distribution function. This automatically ensures the existence of a supplementary conservation law with a concave entropy density which guarantees the hyperbolicity of the resulting system of PDE's. The

form of the maximum entropy distribution function, expanded up to the second order around the partial thermal equilibrium state, is [6,5]

$$f = f_M(1 - \lambda^* - \lambda_i^* c_i - \lambda_{ij}^* c_i c_j - \lambda_{ijk}^* c_i c_j c_k - \lambda_{ijkl}^* c_i c_j c_k c_l$$
$$- \lambda_{ijklm}^* c_i c_j c_k c_l c_m - \lambda_{ijklmn}^* c_i c_j c_k c_l c_m c_n), \quad (2.3)$$

where f_M is a local Maxwellian depending on the partial equilibrium variables n, p and $\boldsymbol{c}(\boldsymbol{k}) = \boldsymbol{v}(\boldsymbol{k}) - \boldsymbol{u}$ is the random velocity. The dependence of the coefficients λ^* on the moments is explicitly given.[5,4] In particular, we get for the first $\boldsymbol{c}$–moments of (2.3)

$$
\begin{aligned}
&\int_{\mathbb{R}^3} f \, d\boldsymbol{k} = n, \\
&\int_{\mathbb{R}^3} c_i f \, d\boldsymbol{k} = 0, \\
&\int_{\mathbb{R}^3} c_i c_j f \, d\boldsymbol{k} = \frac{p}{m^*}\delta_{ij} + \frac{\sigma_{ij}}{m^*} \\
&\int_{\mathbb{R}^3} c_i c_j c_r f \, d\boldsymbol{k} = \frac{6}{5m^*}\boldsymbol{q}_{(i}\delta_{jr)} + \nu\frac{12}{5m^*p}\boldsymbol{q}_{<i}\sigma_{jr>}, \\
&\int_{\mathbb{R}^3} c_i c_j c_r c_r f \, d\boldsymbol{k} = \frac{5p^2}{nm^{*2}}\delta_{ij} + \frac{7p}{nm^{*2}}\sigma_{ij} \\
&\qquad\qquad + \nu\left(\frac{2}{nm^{*2}}\sigma_{ir}\sigma_{rj} + \frac{36}{25}\frac{|\boldsymbol{q}|^2}{m^*p}\delta_{ij} + \frac{112}{25}\frac{q_i q_j}{m^*p}\right).
\end{aligned}
\quad (2.4)
$$

We note that the heat flux $\boldsymbol{q}$ enters quadratically in the fourth order moments. If, however, the expansion of the maximum entropy distribution is stopped at first order this $\boldsymbol{q}$–dependence vanishes.[6] The moments corresponding to this linear closure (in $\boldsymbol{q}$) are obtained from (2.4) by setting $\nu = 0$. The great advantage of the nonlinear closure ($\nu = 1$) compared to the linear one ($\nu = 0$) will be highlighted in the sequel.

The final set of moment equations in the 1–D case is obtained by taking moments $1, v_1, |\boldsymbol{v}|^2, v_1^2 - |\boldsymbol{v}|^2/3, |v|^2 v_1$ of (2.1) and assuming f solves (2.4) with $\boldsymbol{q} = q\boldsymbol{e}_1$ and $\boldsymbol{u} = u\boldsymbol{e}_1$. The quantity σ replaces σ_{11}.

$$\frac{\partial n}{\partial t} + \frac{\partial}{\partial x}(nu) = 0,$$

$$\frac{\partial}{\partial t}(nu) + \frac{\partial}{\partial x}\left(nu^2 + \frac{p}{m^*} + \frac{\sigma}{m^*}\right) + \frac{neE}{m^*} = Q,$$

$$\frac{\partial}{\partial t}\left(nu^2 + \frac{3p}{m^*}\right) + \frac{\partial}{\partial x}\left(nu^3 + \frac{5up}{m^*} + \frac{2\sigma u}{m^*} + \frac{2q}{m^*}\right) + \frac{2neuE}{m^*} = Q_w,$$

$$\frac{\partial}{\partial t}\left(\frac{2}{3}nu^2 + \frac{\sigma}{m^*}\right) + \frac{\partial}{\partial x}\left(\frac{2}{3}nu^3 + \frac{4}{3}\frac{up}{m^*} + \frac{7}{3}\frac{u\sigma}{m^*} + \frac{8}{15}\frac{q}{m^*} + \frac{36}{25m^*p}q\sigma\right)$$

$$+\frac{4neuE}{3m^*} = Q_\sigma,$$

$$\frac{\partial}{\partial t}\left(nu^3 + \frac{5up}{m^*} + \frac{2\sigma u}{m^*} + \frac{2q}{m^*}\right) + \frac{\partial}{\partial x}\left[nu^4 + 5\frac{p^2}{n(m^*)^2} + 7\frac{\sigma p}{n(m^*)^2} + \frac{32}{5}\frac{qu}{m^*}\right.$$

$$\left.+u^2\left(8\frac{p}{m^*} + 5\frac{\sigma}{m^*}\right) + \nu\frac{148}{25}\frac{q^2}{m^*p} + \frac{72}{25}\frac{q\sigma u}{m^*p}\right] + \frac{eE}{m^*}\left(3nu^2 + \frac{5p}{m^*} + \frac{2\sigma}{m^*}\right) = \tilde{Q}.$$

Now in order to close the system, it is necessary to find constitutive relations for the production terms. These may be obtained by using the maximum entropy distribution function in computing the moments of $\mathcal{C}[f]$.[10,19]

In the framework of a hydrodynamical model we assume that the productions are functions of the moments. In gas dynamics the requirement of Galilean invariance determines the general expression for the production terms. In the case of carrier transport in semiconductors such expressions cannot be used for several reasons. On one hand, the momentum and energy of charge carriers are no longer conserved. On the other hand, at variance with gas dynamics, there exists a privileged reference frame, represented by the frame of the crystal. Hereafter we shall write the equations of motion in the frame of the lattice. This enables us to consider the mean velocity of electrons (and consequently the momentum) as a first order quantity.

The production terms for momentum Q and energy flux $\tilde{Q}$ can be represented as linear combinations of J and S (to first order around the state of partial thermal equilibrium)

$$Q = -(aJ + bS)$$
$$\tilde{Q} = -(\tilde{a}J + \tilde{b}S)$$

where $a, b, \tilde{a}, \tilde{b}$ are functions of n, T

$$a(n,T) = c_1^J + c_2^J\frac{T}{T_0} + c_3^J\frac{n}{n_0},$$

$$b(n,T) = c_4^J + c_5^J\frac{T}{T_0} + c_6^J\frac{n}{n_0},$$

$$\tilde{a}(n,T) = c_1^S + c_2^S\frac{T}{T_0} + c_3^S\frac{n}{n_0},$$

$$\tilde{b}(n,T) = c_4^S + c_5^S\frac{T}{T_0} + c_6^S\frac{n}{n_0},$$

with T_0=300 K being the lattice temperature and and $n_0 = 10^{18}$ cm^{-3} a reference density. The coefficients c_i and $\tilde{c}_i$ are given in Table 1. For Q_w and Q_σ we introduce relaxation times τ_w, τ_σ and

$$Q_w = -\frac{1}{\tau_w}\left(nu^2 + 3\frac{p}{m^*} - 3\frac{nk_BT_0}{m^*}\right),$$
$$Q_\sigma = -\frac{1}{\tau_\sigma}\left(\frac{2}{3}nu^2 + \frac{\sigma}{m^*}\right).$$

with T_0 being the lattice temperature as introduced above.

Table 1. Coefficients of the production terms.

	c_1	c_2	c_3	c_4	c_5	c_6
J	-1.2882	2.8757	2.51760	73.7355	-10.5425	-23.5540
S	-0.2978	-0.9299	0.00157	26.6875	2.8013	-1.8204

The relaxation times τ_w, τ_σ are, like the coefficients $a, b, \tilde{a}, \tilde{b}$, functions of the scalar quantities that can be constructed with the moments. Moreover all the transport coefficients may depend on the doping concentration (if scattering with impurities is considered). We obtain the relaxation time for energy by fitting MC data for homogeneous doped silicon in the one dimensional case with the expression

$$\tau_w = a_1 + a_2 r + a_3 \exp(-a_4 r)$$

where $r = W/W_0 - 1$, $W_0 = 3/2nk_BT_0$. By expressing the relaxation times in picosecond, we find

$$\boldsymbol{a} = [0.449544, 0.0000706477, 1.33667, 2.449224],$$

while the relaxation times of the shear can be taken as constant $\tau_\sigma = 0.02$.

More refined models for the production terms are also possible,[4] however, in this article our main concern is the comparison of two different algorithms and therefore we limit ourselves to the above representations.

MC simulations[1,11,25] show that the shear stress σ relaxes much faster to its equilibrium value $\sigma = 0$ than the heat flux q. To simplify the equation we therefore neglect the anisotropic stress σ which leads to a reduced system of four equations. Denoting the vector of unknowns $U = (n, J, W, S)^T$ this system is of the form

$$\frac{\partial U}{\partial t} + \frac{\partial}{\partial x}F_\nu(U) + G(U, E) = r(U),$$
$$\epsilon\frac{\partial^2 \phi}{\partial x^2} = -e(N_D - N_A - n), \quad E = \frac{\partial \phi}{\partial x}$$

where the flux vector is

$$
F_\nu = \begin{pmatrix} nu \\ nu^2 + \dfrac{p}{m^*} \\ \dfrac{m^*}{2}nu^3 + \dfrac{5}{2}pu + q \\ \dfrac{m^*}{2}nu^4 + 4pu^2 + \dfrac{16}{5}uq + \dfrac{5}{2m^*n}p^2 + \nu\dfrac{74}{25}\dfrac{q^2}{p} \end{pmatrix} \tag{2.5}
$$

and $\nu \in \{0, 1\}$ represents linear and nonlinear closure. The electric field term is given by

$$
G(U, E) = \frac{e}{m^*} \begin{pmatrix} 0 \\ nE \\ m^*nuE \\ m^* \left(\dfrac{3}{2}m^*nu^2 + \dfrac{5}{2}p \right) E \end{pmatrix}
$$

and the relaxation term is

$$
r(U) = - \begin{pmatrix} 0 \\ aJ + bS \\ \dfrac{1}{\tau_w} \left(W - \dfrac{3}{2}nk_BT_0 \right) \\ \tilde{a}J + \tilde{b}S \end{pmatrix}. \tag{2.6}
$$

As expected, direct inspection shows that the resulting evolution equations are not Galilean invariant. One of the immediate mathematical consequences is that the hyperbolicity region will depend also on the velocity at variance with the case of the mono atomic gas.[24]

3. Domain of hyperbolicity

To find out the hyperbolicity regions for the linear and the nonlinear closure we will use the same procedure in both cases. By definition, the domain of hyperbolicity is

$$
\mathcal{H}_\nu := \left\{ U = (n, J, W, S)^T \mid dF_\nu(U) \quad \text{has four real eigenvalues} \right\}.
$$

The description of $\mathcal{H}_\nu \subset \mathbb{R}^4$ is simplified a lot by the fact that the characteristic polynomial of dF_ν, and hence the eigenvalues, essentially depend on two dimensionless parameters which are scaled velocity $\hat{u}$ and scaled heat flux $\hat{q}$

$$
\hat{u} = \frac{8}{15} \frac{u}{\sqrt{\dfrac{k_B T}{m^*}}}, \qquad \hat{q} = \frac{37}{25} \frac{q}{m^* n \left(\dfrac{k_B T}{m^*} \right)^{3/2}}.
$$

Indeed, the characteristic polynomial $P(\lambda)$ can be written as

$$
P(\lambda) = \frac{k_B^2 T^2}{(m^*)^2} Q \left(\left(\frac{k_B T}{m^*} \right)^{-\frac{1}{2}} \lambda - \frac{17}{8}\hat{u} - \nu\hat{q} \right) \tag{3.7}
$$

where Q is of the form

$$Q(\xi) = \xi^4 + \alpha(\hat{u}, \hat{q})\,\xi^2 + \beta(\hat{u}, \hat{q})\,\xi + \gamma(\hat{u}, \hat{q}) \tag{3.8}$$

and the coefficients α, β, γ are polynomial expressions in $\hat{u}$ and $\hat{q}$

$$\alpha(\hat{u}, \hat{q}) = \left(-3\,\hat{u}\,\hat{q} - \frac{566}{111}\,\hat{q}^2\right)\nu - \frac{10}{3} - \frac{3}{8}\,\hat{u}^2,$$

$$\beta(\hat{u}, \hat{q}) = \left(-\frac{688}{111}\,\hat{q}^3 - \frac{3}{2}\,\hat{u}^2\,\hat{q} - \frac{616}{111}\,\hat{u}\,\hat{q}^2\right)\nu - \frac{5}{3}\,\hat{u} - \frac{160}{111}\,\hat{q} - \frac{1}{8}\,\hat{u}^3,$$

$$\gamma(\hat{u}, \hat{q}) = \left(-\frac{233}{111}\,\hat{q}^4 - \frac{949}{888}\,\hat{u}^2\,\hat{q}^2 + \frac{70}{37}\,\hat{q}^2 - \frac{3}{16}\,\hat{u}^3\,\hat{q} - \frac{283}{111}\,\hat{u}\,\hat{q}^3\right)\nu$$
$$- \frac{40}{111}\,\hat{u}\,\hat{q} - \frac{5}{24}\,\hat{u}^2 - \frac{3}{256}\,\hat{u}^4 + \frac{5}{3}.$$

If $\xi_i^{(\nu)}(\hat{u}, \hat{q})$ denote the roots of (3.8) then

$$\lambda_i^{(\nu)} = \sqrt{\frac{k_B\,T}{m^*}}\left(\xi_i^{(\nu)}(\hat{u}, \hat{q}) + \frac{17}{8}\,\hat{u} + \nu\hat{q}\right), \qquad i = 1, \ldots, 4$$

are the roots of the characteristic polynomial (3.7), i.e. the characteristic velocities of the system under consideration. Since $T > 0$ and $\hat{u}, \hat{q} \in \mathbb{R}$ the number of real $\lambda_i^{(\nu)}$ and real $\xi_i^{(\nu)}$ is equal. Denoting this number by $N_\nu(\hat{u}, \hat{q})$ we conclude that $\mathcal{H}_\nu$ is essentially determined by the two–dimensional set

$$\mathcal{H}_\nu' := \left\{ (\hat{u}, \hat{q}) \,|\, N_\nu(\hat{u}, \hat{q}) = 4 \right\}. \tag{3.9}$$

To check that $\mathcal{H}_\nu'$ is not empty we consider the point $(\hat{u}, \hat{q}) = (0, 0)$ which corresponds to the state of partial thermodynamical equilibrium. In this case $\alpha = -10/3$, $\beta = 0$, $\gamma = 5/3$, and we find four real roots

$$\xi_{1,2} = \pm\frac{1}{3}\sqrt{15 + 3\sqrt{10}} \approx \pm 1.65,$$

$$\xi_{3,4} = \pm\frac{1}{3}\sqrt{15 - 3\sqrt{10}} \approx \pm 0.78.$$

Since the coefficients of the polynomial depend smoothly on $(\hat{u}, \hat{q})$ we expect that $N_\nu(\hat{u}, \hat{q}) = 4$ in a whole neighborhood of $(0, 0)$. However, if we depart from the partial equilibrium state we might reach a point $(\hat{u}, \hat{q}) \in \partial\mathcal{H}_\nu'$ where the number of real roots drops. In such a point $(\hat{u}, \hat{q})$ the corresponding polynomial Q has a double real root. Denoting this root $\tau \in \mathbb{R}$ we get

$$\xi^4 + \alpha\xi^2 + \beta\xi + \gamma = (\xi - \tau)^2(\xi^2 + \delta\xi + \eta)$$

which yields, after comparing coefficients, $\delta = 2\tau$, $\eta = \alpha + 3\tau^2$ and

$$\beta = -2\alpha\tau - 4\tau^3,$$
$$\gamma = \alpha\tau^2 + 3\tau^4.$$

For the second equation we find four solutions

$$\tau_s(\hat{u}, \hat{q}) = s_1 \frac{1}{6} \sqrt{-6\alpha(\hat{u}, \hat{q}) + s_2 6 \sqrt{\alpha(\hat{u}, \hat{q})^2 + 12\gamma(\hat{u}, \hat{q})}}, \quad s_1, s_2 \in \{-1, 1\}.$$

Inserting this result in the equation for β we get a description of the set of double real zeros of Q in the $(\hat{u}, \hat{q})$–plane

$$D_\nu = \left\{ (\hat{u}, \hat{q}) \,|\, \beta + 2\alpha\tau_s + 4\tau_s^3 \big|_{(\hat{u}, \hat{q})} = 0, \ s \in \{-1, 1\}^2, \ \tau_s(\hat{u}, \hat{q}) \in \mathbb{R} \right\}$$

which contains the boundary $\partial\mathcal{H}'_\nu$. In Figure 1, a plot of the boundary $\partial\mathcal{H}'_0$ for the linear and $\partial\mathcal{H}'_1$ for the nonlinear closure is given. Since $N_\nu(0, 0) = 4$, the con-
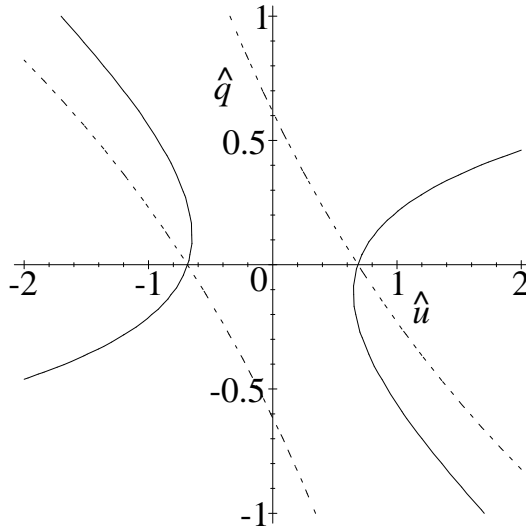
Fig. 1. Hyperbolicity region for the linear (dashed line) and nonlinear closure (continuous line).

nected component containing the origin belongs to $\mathcal{H}'_\nu$ (see Fig. 1). Obviously, the restriction on the heat flux for small velocities in the linear case vanishes altogether if the nonlinear closure is used. As we shall see in Section 6, the hyperbolicity boundary is indeed crossed in standard applications if the linear closure is used. If we cross the boundary $\partial\mathcal{H}'_\nu$ we enter a region with two complex characteristic velocities. This can be checked, for example, by calculating the number of real roots at $(\hat{u}, \hat{q}) = (\pm 2, 0)$.

4. The Kinetic Scheme

Originally, Kinetic Schemes have been used as a tool to solve the compressible Euler equations.[9,18,28,30] The schemes are very natural in the framework of gas dynamics since they are based on the theory of Boltzmann's equation. In fact, they can be viewed as a numerical realization of the famous Hilbert expansion [8]

which states that in the limit of a dense gas solving Boltzmann's equation becomes equivalent to solving the Euler system. Formally this equivalence manifests itself in the fact that the Euler system results from the Boltzmann equation by taking velocity moments under the assumption that the particle distribution is a shifted Maxwellian.

With the hydrodynamical model the situation is quite similar. Here the equations follow from the semiconductor Boltzmann equation if the electrons are close to partial thermodynamical equilibrium and if the corresponding non–equilibrium distribution function is characterized by the first few $\boldsymbol{k}$–moments.

In Section 2, a non–equilibrium distribution has been derived based on the maximum entropy approach. In contrast to its physical interpretation, however, this function may become negative for certain $\boldsymbol{k}$ which is unsatisfactory from a theoretical point of view. Also, to set up a Kinetic Scheme, a nonnegative distribution would be preferable because it assures positivity of even $\boldsymbol{k}$–moments and improves stability. We therefore investigate the question whether it is possible to find a nonnegative distribution function which leads to the nonlinear closure relations of the reduced model. In terms of moments in the peculiar velocity $\boldsymbol{c}(\boldsymbol{k}) = \boldsymbol{v}(\boldsymbol{k}) - \boldsymbol{u}$ this is equivalent to finding a function $f \geq 0$ depending on $n, p, \boldsymbol{q}$ which satisfies (2.4) with $\sigma_{ij} = 0$, i.e.

$$
\begin{aligned}
&\int_{\mathbb{R}^3} f \, d\boldsymbol{k} = n, \\
&\int_{\mathbb{R}^3} c_i f \, d\boldsymbol{k} = 0, \\
&\int_{\mathbb{R}^3} c_i c_j f \, d\boldsymbol{k} = \frac{p}{m^*}\delta_{ij}, \\
&\int_{\mathbb{R}^3} c_i c_j c_r f \, d\boldsymbol{k} = \frac{6}{5m^*}q_{(i}\delta_{jr)}, \\
&\int_{\mathbb{R}^3} c_i c_j c_r c_r f \, d\boldsymbol{k} = 5\frac{p^2}{n(m^*)^2}\delta_{ij} + \frac{36}{25}\frac{|\boldsymbol{q}|^2}{m^* p}\delta_{ij} + \frac{112}{25}\frac{q_i q_j}{m^* p}.
\end{aligned}
\tag{4.10}
$$

It can be shown that (4.10) is in fact solvable provided n, p are positive.[17]

For a practical construction of a solution to (4.10) we use certain scaling and symmetry properties. It turns out that (4.10) can be reduced to the easier moment problem to find $g_{\gamma,\delta} : \mathbb{R} \times \mathbb{R}^+ \mapsto \mathbb{R}^+$ which satisfies

$$
\int_{\mathbb{R} \times \mathbb{R}^+} P(\boldsymbol{w})g_{\gamma,\delta}(\boldsymbol{w}) \, d\boldsymbol{w} = \rho(\gamma, \delta),
\tag{4.11}
$$

with the polynomial vector

$$
P(\boldsymbol{w}) = (\, w_2\,,\, w_1 w_2,\, w_1^2 w_2,\, w_2^3,\, w_1 w_2^3,\, w_1^3 w_2,\, w_1^2 w_2(w_1^2 + w_2),\, w_2^3(w_1^2 + w_2)\,)^T,
$$

and the moments

$$
\rho(\gamma, \delta) = (1, 0, 1, 2, 2\gamma, 3\gamma, 5 + 37\delta, 10 + 18\delta)^T, \qquad \gamma, \delta \in \mathbb{R}.
$$

The relation between (4.10) and (4.11) is clarified in the following

Lemma 1   *Let $n, T > 0$ and let $R \in SO(3)$ be a rotation matrix which satisfies $R^{-1}\boldsymbol{q} = |\boldsymbol{q}|\boldsymbol{e}_1$, where $\boldsymbol{e}_1$ is the first standard basis vector in $\mathbb{R}^3$. For abbreviation we set $\vartheta = k_B T / m^*$. Let g_{γ,γ^2} be a solution of (4.11) with*

$$\gamma = \frac{2|\boldsymbol{q}|}{5m^* n \vartheta^{\frac{3}{2}}}.$$

Then

$$f(\boldsymbol{k}) := \frac{n}{\left(\frac{m^*}{\hbar}\sqrt{\vartheta}\right)^3} f^* \left(\frac{1}{\sqrt{\vartheta}} R^{-1} c(\boldsymbol{k}) \right)$$

with

$$f^*(\boldsymbol{\xi}) := \frac{1}{2\pi} g_{\gamma,\gamma^2} \left(\xi_1, \sqrt{\xi_2^2 + \xi_3^2} \right)$$

is a solution of the original problem (4.10).

We note that (4.11) puts only eight conditions on g_{γ,γ^2} where γ is a scalar parameter in contrast to 26 conditions in (4.10) which depend on five variables $n, p, \boldsymbol{q}$. A further simplification can be achieved by writing g_{γ,γ^2} in the form

$$g_{\gamma,\gamma^2} = \sum_{i=1}^{M} \lambda_i(\gamma) g_{\gamma_i,\delta_i}, \qquad \lambda_i(\gamma) \geq 0. \tag{4.12}$$

The functions g_{γ_i,δ_i} are solutions of (4.11) where the parameters $\lambda_i, \gamma_i, \delta_i$ are chosen such that

$$\begin{pmatrix} \gamma \\ \gamma^2 \end{pmatrix} = \sum_{i=1}^{M} \lambda_i(\gamma) \begin{pmatrix} \gamma_i \\ \delta_i \end{pmatrix}.$$

With this approach it is possible to reduce (4.10) to a finite number of problems of type (4.11). Once the densities g_{γ_i,δ_i} are determined, a non–equilibrium distribution f can be set up using (4.12) and Lemma 1.

To solve (4.11) for a pair (γ, δ) we use the ansatz

$$g_{\gamma,\delta}(\boldsymbol{w}) = \sum_{j=1}^{N} \frac{\alpha_j}{\tau_j^2} \Phi \left(\frac{\boldsymbol{w} - \boldsymbol{\omega}_j}{\tau_j} \right), \qquad \alpha_j \geq 0 \tag{4.13}$$

where $\Phi \geq 0$ is a given density, τ_j are fixed scaling constants and $\boldsymbol{\omega}_j$ are prescribed shifting vectors. Inserting (4.13) into (4.11) leads to the linear programming problem

$$A\alpha = \rho(\gamma, \delta) \qquad 0 \leq \alpha \in \mathbb{R}^N$$

with $A \in \mathbb{R}^{8 \times N}$ given by

$$A_{ij} = \int_{\mathbb{R} \times \mathbb{R}^+} P_i(\boldsymbol{w}) \frac{1}{\tau_j^2} \Phi \left(\frac{\boldsymbol{w} - \boldsymbol{\omega}_j}{\tau_j} \right) d\boldsymbol{w}.$$

With a dense grid of shifting vectors $\boldsymbol{\omega}_j$ the dimension of the problem can easily become as large as $N = 10\,000$. Nevertheless, the simplex algorithm returns a solution vector α with at most eight nonzero components.[21] With the non–equilibrium distribution at hand we can now derive the Kinetic Scheme.

In a 1–D situation we assume that all quantities depend only on the first coordinate $x \in (0, L)$ and that particle and energy flux are of the form $J\boldsymbol{e}_1$, $S\boldsymbol{e}_1$. We denote the vector of unknowns by $U = (n, J, W, S)^T$ and the non–equilibrium distribution by $f(U; \boldsymbol{k})$.

As already mentioned, the Kinetic Scheme uses the fact that the reduced hydrodynamical model can be derived from the Boltzmann equation

$$\partial_t \varphi + v_1 \partial_x \varphi - \frac{q}{\hbar} E[\varphi] \partial_{k_1} \varphi = \mathcal{C}[\varphi],$$
$$\partial_x E = \frac{e}{\varepsilon_s} \left(N_D - N_A - \int_{\mathbb{R}^3} \varphi \, d\boldsymbol{k} \right), \tag{4.14}$$

by taking moments with respect to $1, v_1, \frac{m}{2}|\boldsymbol{v}|^2, \frac{m}{2}|\boldsymbol{v}|^2 v_1$ and assuming that φ is the non–equilibrium distribution. The latter condition will not be violated too much if we solve (4.14) with the initial value $\varphi(x, \boldsymbol{k}, 0) = f(U^0(x); \boldsymbol{k})$ for a small time step Δt where U^0 are the initial moments. At the end of the time step we calculate the new moments U^1 and reinitialize φ according to $\varphi(x, \boldsymbol{k}, \Delta t) = f(U^1(x); \boldsymbol{k})$. The whole process can be iterated and the re-initialization makes sure that φ does not depart too far from the set of non–equilibrium distributions.

To analyze the resulting scheme for the moments of φ let us consider the first time step. Due to the nonlinear term $E[\varphi] \partial_{k_1} \varphi$ as well as the complicated collision kernel $\mathcal{C}[\varphi]$ we cannot hope for an explicit solution of (4.14). We will therefore resort to an approximate solution which we obtain by a standard splitting approach. Separating the transport part of (4.14) from the collision process leads to a Vlasov–Poisson problem which we immediately simplify further by exchanging $E[\varphi^{(1)}]$ with the initial electric field $E^0(x)$. We get the linear problem

$$\partial_t \varphi^{(1)} + v_1 \partial_x \varphi^{(1)} - \frac{q}{\hbar} E^0(x) \partial_{k_1} \varphi^{(1)} = 0,$$
$$\partial_x E^0 = \frac{e}{\varepsilon_s}(N_D - N_A - n^0), \tag{4.15}$$
$$\varphi^{(1)}(x, \boldsymbol{k}, 0) = f(U^0(x); \boldsymbol{k}).$$

The resulting moment vector is denoted

$$M(x, t) := \int_{\mathbb{R}^3} P(\boldsymbol{k}) \varphi^{(1)}(x, \boldsymbol{k}, t) \, d\boldsymbol{k}, \qquad P(\boldsymbol{k}) = \begin{pmatrix} 1 \\ v_1 \\ \frac{m}{2}|\boldsymbol{v}|^2 \\ \frac{m}{2}|\boldsymbol{v}|^2 v_1 \end{pmatrix}. \tag{4.16}$$

The collision process is then taken care of by a space homogeneous Boltzmann equation

$$\partial_t \varphi^{(2)} = \mathcal{C}[\varphi^{(2)}]. \tag{4.17}$$

In the derivation of the hydrodynamical model the moment integrals of the collision operator have been approximated by relaxation–type expressions involving moments of the electron distribution. Hence, on the level of moments, (4.17) turns into a system of ODEs

$$\begin{cases} \dfrac{\partial}{\partial t} U = r(U), \\ U(x,0) = M(x, \Delta t) \end{cases} \tag{4.18}$$

with r defined in (2.6). While (4.18) can be treated with standard methods, the transport part (4.15) is the actual kinetic step of the scheme. We will solve (4.15) with the method of characteristics which is based on the fact that $\varphi^{(1)}$ is constant along the curves given by

$$\dot{x} = v_1 = \frac{\hbar}{m^*} k_1, \qquad \dot{k}_1 = -\frac{e}{\hbar} E^0(x), \qquad \dot{k}_2 = 0, \qquad \dot{k}_3 = 0. \tag{4.19}$$

The solution of (4.19) with initial value $(x, \boldsymbol{k})$ is denoted by $t \mapsto \mathcal{T}_t(x, \boldsymbol{k}) = (X_t(x, \boldsymbol{k}), K_t(x, \boldsymbol{k}))$. If the space curve $t \mapsto X_t(x, \boldsymbol{k})$ stays inside $(0, L)$ we know that $\varphi^{(1)}(x, \boldsymbol{k}, \Delta t)$ is determined by the initial condition. Otherwise, the entrance time

$$\eta(x, \boldsymbol{k}) := \{\, t > 0 \,|\, X_{-t}(x, \boldsymbol{k}) \in \{0, L\} \,\}$$

is less than Δt and $\varphi^{(1)}(x, \boldsymbol{k}, \Delta t)$ depends on the boundary values. If the density $\beta^0(x, \boldsymbol{k})$ describes the distribution of incoming electrons during the first time step we obtain

$$\varphi^{(1)}(x, \boldsymbol{k}, \Delta t) = \begin{cases} \beta^0(\mathcal{T}_{-\eta}(x, \boldsymbol{k})) & \eta = \eta(x, \boldsymbol{k}) \le \Delta t, \\ f(U^0(X_{-\Delta t}(x, \boldsymbol{k})); K_{-\Delta t}(x, \boldsymbol{k})) & \eta(x, \boldsymbol{k}) > \Delta t \end{cases} .$$

Using a local approximation of the characteristic flow

$$\mathcal{T}_{\Delta t}(x, \boldsymbol{k}) \approx \left(x + v_1 \Delta t, k_1 - \frac{e}{\hbar} E_j^0 \Delta t, k_2, k_3 \right)$$

we find an approximate expression for the cell averages of M in standard form

$$M_j^1 = U_j^0 - \frac{\Delta t}{\Delta x_j} \left(F_{j+\frac{1}{2}}^0 - F_{j-\frac{1}{2}}^0 \right) - \Delta t G_j^0. \tag{4.20}$$

Here Δx_j is the length of the jth discretization cell $[x_{j-\frac{1}{2}}, x_{j+\frac{1}{2}}]$, U_j^0 the corresponding cell average of the initial value and E_j^0 approximates E^0 in the cell center. The production term G_j^0 is given by

$$G_j^0 = \frac{1}{\Delta t} \int_{\mathbb{R}^3} \left(P(\boldsymbol{k}) - P\left(\boldsymbol{k} + \Delta \boldsymbol{k}_j^0 \right) \right) f(U_j^0; \boldsymbol{k}) \, d\boldsymbol{k}$$

where $\Delta \boldsymbol{k}_j^0 = -\frac{e}{\hbar} E_j^0 \Delta t \boldsymbol{e}_1$ is the change in the $\boldsymbol{k}$–vector induced by the field E_j^0. The numerical flux $F_{j+\frac{1}{2}}^0$ splits into contributions in positive and negative x–direction

$$F_{j+\frac{1}{2}}^0 = (F^+)_{j+\frac{1}{2}}^0 + (F^-)_{j+\frac{1}{2}}^0. \tag{4.21}$$

While the incoming fluxes at the boundary depend on β^0

$$(F^+)^0_{\frac{1}{2}} = \int_{k_1>0} v_1(\boldsymbol{k})P(\boldsymbol{k})\beta^0(0,\boldsymbol{k})\,d\boldsymbol{k},$$

$$(F^-)^0_{N+\frac{1}{2}} = \int_{k_1<0} v_1(\boldsymbol{k})P(\boldsymbol{k})\beta^0(L,\boldsymbol{k})\,d\boldsymbol{k}$$

we have for the remaining fluxes

$$(F^+)^0_{j+\frac{1}{2}} = \int_{k_1>0} v_1(\boldsymbol{k})P\left(\boldsymbol{k}+\Delta\boldsymbol{k}^0_j\right) f(U^0_{j+};\boldsymbol{k})\,d\boldsymbol{k},$$

$$(F^-)^0_{j+\frac{1}{2}} = \int_{k_1<0} v_1(\boldsymbol{k})P\left(\boldsymbol{k}+\Delta\boldsymbol{k}^0_{j+1}\right) f(U^0_{(j+1)-};\boldsymbol{k})\,d\boldsymbol{k}.$$

The moments U^0_{j+}, U^0_{j-} are approximations of U^0 at the points $x_{j+} = x_{j+\frac{1}{2}} - \frac{1}{2}\Delta x_{\min}$ and $x_{j-} = x_{j-\frac{1}{2}} + \frac{1}{2}\Delta x_{\min}$. We use linear interpolation

$$U^0_{j+} := \frac{x_{j+}-x_j}{x_{j+1}-x_j}U^0_{j+1} + \frac{x_{j+1}-x_{j+}}{x_{j+1}-x_j}U^0_j,$$

$$U^0_{j-} := \frac{x_j-x_{j-}}{x_j-x_{j-1}}U^0_{j-1} + \frac{x_{j-}-x_{j-1}}{x_j-x_{j-1}}U^0_j,$$

respectively extrapolation

$$U^0_{1-} := U^0_1 + \frac{U^0_2 - U^0_1}{x_2 - x_1}(x_{1-} - x_1),$$

$$U^0_{N+} := U^0_N + \frac{U^0_N - U^0_{N-1}}{x_N - x_{N-1}}(x_{N+} - x_N).$$

Please note that on a regular grid $\Delta x_j = \Delta x_{\min}$ for all j so that $x_{j-} = x_j = x_{j+}$ and hence $U^0_{j-} = U^0_j = U^0_{j+}$. If all particle densities are supported on $|k_1| \leq \frac{m^*}{\hbar}v_{\max}$ then the CFL–like condition

$$v_{\max}\Delta t \leq \Delta x_{\min} \tag{4.22}$$

ensures positivity of number density, energy and temperature after the transport step[17] (at least on the finest part of the grid where $\Delta x_j = \Delta x_{\min}$). One reason for this is the structure of the numerical flux which also includes the electric field terms $\Delta\boldsymbol{k}^0_j$. On the other hand, this structure implies that the usual consistency relation for the numerical flux is violated. However, since $\Delta\boldsymbol{k}^0_j$ are of order Δt we can show that the complete scheme consisting of transport step and collision step is first order consistent to the reduced hydrodynamical model.[17]

In order to increase the accuracy of the scheme, especially near junctions in the doping profile where steep gradients are encountered, we use a locally refined grid.

The numerical results in Section 6 are based on a partial equilibrium distribution $f(U;\boldsymbol{k})$ which consists of a sum of Dirac–delta measures, i.e. $\Phi(\boldsymbol{w}) = \delta_0(\boldsymbol{w})$ in (4.13). As far as the evaluation of the production terms G^0_j and the fluxes $F^0_{j+\frac{1}{2}}$ is concerned, this is certainly the easiest choice. As boundary value β^0 we use

$f(U_{1+}^0; \boldsymbol{k})$ and $f(U_{N-}^0; \boldsymbol{k})$ respectively. This choice ensures that in the terminal cells incoming and outgoing fluxes compensate approximately.

5. Finite difference scheme

We compare the numerical results obtained by the Kinetic Scheme with those obtained by a difference scheme. The scheme that we use is a finite difference scheme, where the hyperbolic step is solved by a second order shock-capturing central scheme,[26] and a relaxation step takes care of the relaxation and drift effects. We rewrite the system of evolution equations in the form

$$\frac{\partial U}{\partial t} + \frac{\partial}{\partial x} F_\nu(U) = r(U) - G(U, E) \tag{5.23}$$

coupled with Poisson's equation

$$\epsilon \frac{\partial^2 \phi}{\partial x^2} = -e(N_D - N_A - n), \quad E = \frac{\partial \phi}{\partial x} \tag{5.24}$$

The basic splitting scheme is obtained as follows: given the field variable U^n at time t_n,

- solve Poisson's equation $E^n = \mathcal{P}(U^n)$

- solve the relaxation step

$$\frac{\partial \tilde{U}}{\partial t} = r(\tilde{U}) - G(\tilde{U}, E^n), \quad t \in [0, \Delta t]; \quad \tilde{U}(0) = U^n$$

- solve the convection step

$$\frac{\partial \hat{U}}{\partial t} + \frac{\partial F_\nu(\hat{U})}{\partial x} = 0, \quad t \in [0, \Delta t]; \quad \hat{U}(0) = \tilde{U}(\Delta t)$$

- set $U^{n+1} = \hat{U}(\Delta t)$

Remarks   The splitting used here is quite different than the one used in the Kinetic Scheme. Here, for example, relaxation and drift effects are described by the relaxation step. Poisson's equation is discretized by finite differences and solved by a standard tridiagonal solver. The relaxation step is solved by an implicit scheme, in order to avoid stability restriction on the time step. The convection step is solved using the Nessyahu-Tadmor scheme, which is second order in space and time. We shall describe separately the discrete relaxation and convection steps.

5.1. *Relaxation step*

The relaxation equations take the form

$$\frac{\partial n}{\partial t} = 0,$$

$$\frac{\partial J}{\partial t} = -(aJ + bS) - enE,$$

$$\frac{\partial W}{\partial t} = -\frac{1}{\tau_w}\left(W - \frac{3}{2}nk_BT_0\right) - envE,$$

$$\frac{\partial S}{\partial t} = -(\tilde{a}J + \tilde{b}S) - \frac{eE}{2}(3m^*nv^2 + 5p).$$

By evaluating the relaxation times and the electric field at $t = t_n$, we can numerically integrate the previous equations. For density and energy we easily have

$$n_j^{n+1} = n_j^n,$$

$$W_j^{n+1} = \frac{3}{2}n_j^n k_B T_0 + \left(W_j^n - \frac{3}{2}n_j^n k_B T_0\right)\exp\left(-\frac{\Delta t}{\tau_{wj}^n}\right)$$
$$-J_j^n e E_j^n \tau_w j\left[1 - \exp\left(\frac{-\Delta t}{\tau_{Wj}^n}\right)\right].$$

The equations for the momentum and energy flux can be rewritten as

$$\frac{dV}{dt} = -AV + C,$$

where

$$V = \begin{pmatrix} J \\ S \end{pmatrix}, \quad C = \begin{pmatrix} c_1 \\ c_2 \end{pmatrix} = \begin{pmatrix} -en_j^n E_j^n \\ -\frac{eE_j^n}{2}(3m^*n_j^n(v_j^n)^2 + 5p_j^n) \end{pmatrix}, \quad A = \begin{pmatrix} a & b \\ \tilde{a} & \tilde{b} \end{pmatrix}.$$

By integrating we have

$$V_j^{n+1} = BV_j^n - (B - I)C,$$

with

$$B = Q\exp(-\Lambda\Delta t)Q^{-1} = Q\,\text{diag}\left(\exp(-\lambda_1\Delta t), \exp(-\lambda_2\Delta t)\right)Q^{-1}$$

λ_1 and λ_2 being the eigenvalues of A and Q the matrix of the right eigenvector of A.

5.2. *Convection step*

The convection step has the structure of a quasilinear hyperbolic system of conservation laws. It is well known that the solutions of such systems suffer loss of regularity and may develop discontinuities. Several schemes have been designed for the numerical approximation of such systems (see[14] for a review on modern shock capturing schemes).

Higher order upwind methods have been developed, and used for solving problems in semiconductor device simulation, such as ENO schemes.[27] These schemes,

however, require an exact or approximate Riemann solver, or at least the knowledge of the characteristic structure of the Jacobian matrix. For systems similar to gas dynamics, an approximate Riemann solver based on the Roe matrix is used. Hence, the upwind approach is suitable when analytical expressions for the eigenvalues and eigenvectors are known explicitly. In the model considered here, no simple analytical expressions for the eigenvalues are known. Therefore, it is desirable to use a shock-capturing scheme that does not require the explicit knowledge of the characteristic structure of the system. Two families of schemes have this property: relaxation schemes,[15] and central schemes.[26] Both schemes are simple and robust. The last one does not require the computation of the Jacobian matrix. Its building block is the Lax-Friedrichs scheme, corrected by a MUSCL type interpolation that guarantees second order in smooth regions and TVD property.[33] For the sake of completeness, we report the derivation of NT scheme and UNO reconstruction (for more details, we refer to the articles by Nessyahu and Tadmor[26] and Harten and Osher[12]).

Let us consider a system of the form

$$\frac{\partial v}{\partial t} + \frac{\partial F(v)}{\partial x} = 0, \tag{5.25}$$

where $v \in \mathbb{R}^m$ and $F : \mathbb{R}^m \to \mathbb{R}^m$. We introduce a uniform spatial grid $x_1, x_2, \cdots, x_N$, and a temporal discretization $t_n = n\Delta t$. By integrating Eq. (5.25) on a cell $[x_j, x_{j+1}] \times [t_n, t_{n+1}]$, one obtains

$$\overline{v}_{j+\frac{1}{2}}(t_n + \Delta t) = \overline{v}_{j+\frac{1}{2}}(t_n)$$
$$- \frac{1}{\Delta x} \left[\int_{t_n}^{t_n+\Delta t} F(v(x_{j+1}, \tau)) d\tau - \int_{t_n}^{t_n+\Delta t} F(v(x_j, \tau)) d\tau \right], \tag{5.26}$$

where

$$\overline{v}_{j+\frac{1}{2}}(t_n) = \frac{1}{\Delta x} \int_{x_j}^{x_{j+1}} v(y, t_n) dy$$

represents the cell average of $v(x,t)$ in $[x_j, x_{j+1}]$ for $t = t_n$. The integral of the flux $F(v(x,t))$ is computed by the midpoint quadrature rule:

$$\int_{t_n}^{t_n+\Delta t} F(v(x_j, \tau)) d\tau = \Delta t\, F\left(v\left(x_j, t_n + \frac{\Delta t}{2} \right) \right) + O(\Delta t^3). \tag{5.27}$$

The quantity $v(x_j, t_n + \Delta t/2)$, is computed according to the Lax-Wendroff approach, by using Taylor's formula:

$$v\left(x_j, t + \frac{\Delta t}{2} \right) = v_j(t) - \frac{1}{2}\lambda F'_j + O(\Delta t^2),$$

where $F'_j/\Delta x$ is an approximation of the derivative of the flux (yet to be specified), and $\lambda = \frac{\Delta t}{\Delta x}$. In order to obtain a second order scheme we require that

$$\frac{1}{\Delta x} F'_j = \left. \frac{\partial}{\partial x} F(v(x,t)) \right|_{x=x_j} + O(\Delta x).$$

By substituting (5.27) into (5.26), one has a relation that involves both cell averages and point values of the solution.

By introducing a MUSCL interpolation, we approximate $v(x, t)$ by a piecewise linear polynomial

$$L_j(x, t) = v_j(t) + (x - x_j) \frac{1}{\Delta x} v_j', \qquad x_{j-\frac{1}{2}} \leq x \leq x_{j+\frac{1}{2}}.$$

and in order to ensure a second order accuracy we require that

$$\frac{1}{\Delta x} v_j' = \left. \frac{\partial}{\partial x} v(x, t) \right|_{x = x_j} + O(\Delta x). \tag{5.28}$$

Therefore, Eq. (5.28) gives

$$v_{j+\frac{1}{2}}(t + \Delta t) = \frac{1}{2} \left[v_j(t) + v_{j+1}(t) \right] + \frac{1}{8} \left[v_j' - v_{j+1}' \right] +$$
$$- \lambda \left[F\left(v_{j+1}(t) - \frac{1}{2} \lambda F_{j+1}' \right) - F\left(v_j(t) - \frac{1}{2} \lambda F_j' \right) \right] + O(\Delta t^3).$$

Because the initial state at $t = t_n$ is given by the piecewise linear function $L_j(x, t_n)$, the fluxes remain regular functions if the solution to the corresponding generalized Riemann problems between adjacent cells do not interact.

This is obtained by imposing the following CFL condition

$$\lambda \cdot \max \rho(A(v(x, t))) < \frac{1}{2} \tag{5.29}$$

where $\rho(A(v(x, t)))$ is the spectral radius of the Jacobian matrix,

$$A = \frac{\partial F}{\partial v}.$$

In this way a family of predictor-corrector schemes is obtained:

$$v_j^{n+\frac{1}{2}} = v_j^n - \frac{1}{2} \lambda F_j',$$
$$v_{j+\frac{1}{2}}^{n+1} = \frac{1}{2} \left[v_j^n + v_{j+1}^n \right] - \lambda \left[g_{j+1} - g_j \right],$$

where

$$g_j = F(v_j^{n+\frac{1}{2}}) + \frac{1}{8\lambda} v_j'.$$

Such schemes are conservative and consistent, which is a necessary requirement for correct shock capturing.

In order to determine the expression of v_j' and F_j', we make use of a Uniform Non Oscillatory reconstruction,[12] which guarantees uniform second order accuracy (even near local extrema) for smooth solutions.

Starting from the cell average of $v(x,t)$, one constructs a piecewise quadratic polynomial $Q(x,t)$, such that

$$
\begin{aligned}
Q(x_j, t) &= v(x_j, t) + O(\Delta x^3), \\
\frac{d}{dx}Q(x \pm 0, t) &= \frac{dv(x,t)}{dx} + O(\Delta x^2),
\end{aligned}
$$

when $v(x,t)$ is a regular function.

The required condition on $Q(x,t)$ is to be non oscillatory, in the sense that its number of local extrema is not larger than that of $v(x,t)$. This is obtained with an appropriate choice of the stencil.

For $x_j \le x \le x_{j+1}$, the two candidates to $Q(x,t)$ are the polynomial interpolating the function on the nodes x_{j-1}, x_j, x_{j+1}, and the one interpolating the function on the nodes x_j, x_{j+1}, x_{j+2}. The one which is closer to the line through points $(x_j, v(x_j, t))$ and $(x_{j+1}, v(x_{j+1}, t))$ is chosen.

In the interval $x_j \le x \le x_{j+1}$ we write

$$
Q(x, \cdot) = v_j + d_{j+\frac{1}{2}}v\frac{x - x_j}{\Delta x} + \frac{1}{2}D_{j+\frac{1}{2}}v\frac{(x - x_j)(x - x_{j+1})}{(\Delta x)^2},
$$

with

$$
d_{j+\frac{1}{2}}v = v_{j+1} - v_j.
$$

Then one has

$$
D_{j+\frac{1}{2}}v = v_{j+1} - 2v_j + v_{j-1}
$$

if we choose x_{j-1}, x_j, x_{j+1}, and

$$
D_{j+\frac{1}{2}}v = v_{j+2} - 2v_{j+1} + v_j
$$

if we choose x_j, x_{j+1}, x_{j+2}.

This choice can be expressed in the form

$$
D_{j+\frac{1}{2}}v = MM(v_{j+2} - 2v_{j+1} + v_j, v_{j+1} - 2v_j + v_{j-1}) \tag{5.30}
$$

where $MM(x,y)$ is the min mod function, defined by

$$
MM(x, y) = \begin{cases} sgn(x) \cdot \min(|x|, |y|) & \text{if } sgn(x) = sgn(y) \\ 0 & \text{otherwise.} \end{cases}
$$

We can compute the slope of $L_j(x,t)$ by

$$
\frac{v_j'}{\Delta x} = MM\left(\frac{d}{dx}Q(x_j - 0, t), \frac{d}{dx}Q(x_j + 0), t)\right).
$$

that is by

$$
v_j' = MM\left(d_{j-\frac{1}{2}}v + \frac{1}{2}MM(D_{j-1}, D_j), d_{j+\frac{1}{2}}v - \frac{1}{2}MM(D_j, D_{j+1})\right) \tag{5.31}
$$

where

$$D_j = v_{j+1} - 2v_j + v_{j-1}.$$

The computation of F_j' can be obtained by a similar reconstruction, from the values of $F(\overline{v}_j^n)$ or by the Jacobian matrix

$$F_j' = \frac{\partial F}{\partial v}(v_j)v_j'.$$

Because of the staggered grid, we perform the convection step by two NT steps, so that the field for the relaxation step is computed on a non staggered grid.

5.3. *Second order splitting*

The basic splitting scheme introduced at the beginning of the section is not second order accurate in time, and the loss of accuracy is apparent even when computing stationary solutions. To improve accuracy, other methods like Strang splitting[31] could be applied. Here, however, we use a different technique[20] which we found more accurate, and which does not require a second order approximation of the relaxation step.

The scheme is given as follows: starting with the fields (U^n, E^n) at time t_n, the fields at time t_{n+1} are obtained as

$$
\begin{aligned}
U_1 &= U^n - R(U_1, E^n, \Delta t), \\
U_2 &= \frac{3}{2}U^n - \frac{1}{2}U_1, \\
U_3 &= U_2 - R(U_3, E^n, \Delta t), \\
U_4 &= \mathcal{C}_{\Delta t}U_3, \\
E^{n+1} &= \mathcal{P}(U_4), \\
U^{n+1} &= U_4 - R(U^{n+1}, E^{n+1}, \Delta t/2)
\end{aligned}
$$

where R represents the numerical operator corresponding to relaxation step, $\mathcal{C}_{\Delta t}$ represents the numerical convection operator corresponding to two steps of NT scheme, $\mathcal{P}(U)$ gives the solution of Poisson's equation.

6. Numerical Results

As test problem we consider a ballistic silicon diode $n^+ - n - n^+$, which models a MOSFET channel. We shall integrate the equations representing the nonlinear model by using both the kinetic and the finite difference method presented in the previous sections.

The values of the physical constants are the following. The bulk temperature is supposed to be $300°$K. The n^+ regions are $0.1\mu m$ long with a donor density $N_D^+ = 0.5n_0 = 5 \cdot 10^{17} cm^{-3}$. The channel has length $L_c = 0.4\mu m$ with a doping density $N_D = 0.002n_0$ which leads to a jump factor 250 at the junctions. For the electron effective mass in the parabolic band approximation we use $m^* = 0.32 \; m_e$, m_e being the electron mass. The dielectric constant of silicon is given by $\epsilon = \epsilon_r \epsilon_0$, where $\epsilon_r = 11.7$ is the relative dielectric constant and $\epsilon_0 = 8.85 \times 10^{-18} C/V \mu m$ is the dielectric constant of vacuum.

A bias voltage V_b=1 Volt is considered and the doping profile is regularized according to the function

$$ n_0(x) = N_D^+ - \frac{N_D^+ - N_D}{2} \left(\tanh \frac{x - x_1}{s} - \tanh \frac{x - x_2}{s} \right), $$

where $s = 0.01\mu$m, $x_1 = 0.1\mu$m, and $x_2 = x_1 + L_c$. The total length of the device is $L = L_c + 0.2\mu$m.

The initial conditions for the system are

$$ n(x,0) = n_0(x), \quad T(x,0) = 300°\text{K}, \quad v(x,0) = 0, \quad q(x,0) = 0. \qquad (6.32) $$

Regarding the boundary conditions, in principle the number of independent conditions on each boundary should be equal to the number of characteristics entering the domain. However, in the highly doped regions one is close to thermodynamic equilibrium, therefore in that part of the device the nonlinear effects are negligible and the results should be very close to those obtained for the iterated model[29] (which is obtained by applying to a Maxwellian iteration to the closure relations given by the extended thermodynamics approach[2]). Numerical results for the iterated model show that the solution is flat near the boundary. This justifies the use of the following boundary conditions

$$
\begin{aligned}
n(0,t) &= n(L,t) = N_D^+ \\
\frac{\partial J}{\partial x}(0,t) &= \frac{\partial J}{\partial x}(L,t) = 0, \\
\frac{\partial W}{\partial x}(0,t) &= \frac{\partial W}{\partial x}(L,t) = 0, \\
\frac{\partial S}{\partial x}(0,t) &= \frac{\partial S}{\partial x}(L,t) = 0.
\end{aligned}
$$

Since there is no sign of spurious oscillations near the boundary, the boundary conditions turn out to be compatible with the solution of the problem. Finally, the

boundary conditions for the electric potential are given by

$$e\phi(0) = T_0 \ln\left(\frac{n(0)}{n_i}\right), \qquad e\phi(L) = T_0 \ln\left(\frac{n(L)}{n_i}\right) + eV_b,$$

where $n_i = 1.4 \times 10^{10}$ cm^{-3} is electron intrinsic concentration, and V_b is the applied bias voltage.

In all calculations, the stationary solution is reached within a few picoseconds. Because a stable scheme has been used for the relaxation step, the only stability restriction on the time step is given by the convection step. In all simulations the stability condition (5.29) respectively (4.22) is always satisfied.

In the stationary case the continuity equation reduces to

$$\partial_x J = 0,$$

that is the current should be constant along the device for smooth solutions. However both methods give numerical solutions with deviation from constant flux near the junctions. Of course the used schemes approximate a modified equation $\partial_t n + \partial_x J = \Xi$ to a higher order. The term Ξ represents the numerical viscosity added by the method. It is relative large at the junctions (especially at the second one) where n has steep gradients. The deviations should decrease by increasing the number of grid points. In order to analyze this behavior we perform calculations with different mesh sizes. In Figure 2 the value of J is shown for the solutions obtained with the
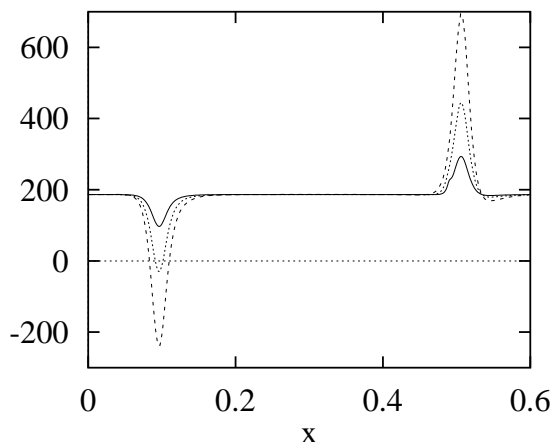
Fig. 2. Values of the current eJ on a regular grid with 200 (dashed line) and 400 (dotted line) points and on a locally refined grid with 400 points (solid line) by using the Kinetic Scheme.

Kinetic Scheme on a regular grid of 200 and 400 cells and on a locally refined grid with 400 cells. It is evident that the momentum has a smaller deviation when a finer grid is used. In Fig.3 the value of J is reported for the numerical solution obtained with the finite difference method when 400 and 800 cells are taken. Concerning the first junction we find a similar behavior but in the second one, even after increasing
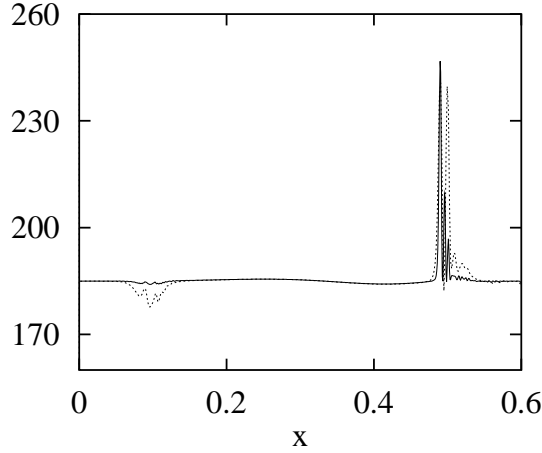
Fig. 3. Values of the current eJ obtained with the finite difference scheme based on 400 (dotted) and 800 points (solid).

the number of grid points, some irregularities are still present. With 800 the momentum is practically conserved along all the device but in the second junction a spike of small size remains. This suggests that in the second junction there could be the presence of an irregularity more singular than a shock, e.g. a delta–shock.[32] Of course such an assessment requires a more detailed analysis and we do not pursue it any more in this paper. The only remark is that this effect is more evident with the
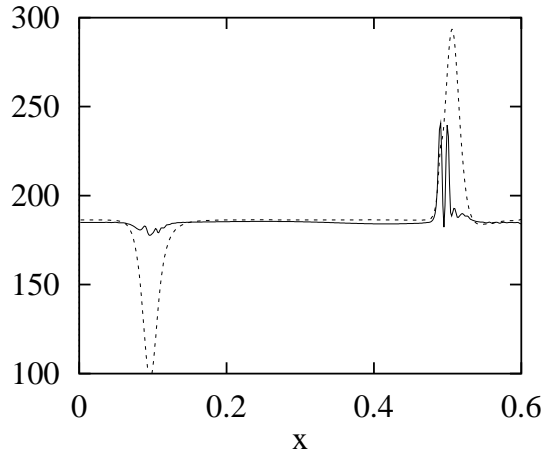
Fig. 4. Current eJ in $Cs^{-1}mm^{-2}$ obtained with Kinetic Scheme (dashed) and finite difference scheme (solid).

finite difference method because it is second order accurate (see Fig. 4). Concerning the results of the other fields (velocity, energy, heat flux and electric field) they are shown in the remaining Figures 5,6,7,8. The finite difference scheme (solid line) which is based on a regular grid of 400 points is compared with the Kinetic Scheme (dashed line) based on a locally refined grid of 400 points
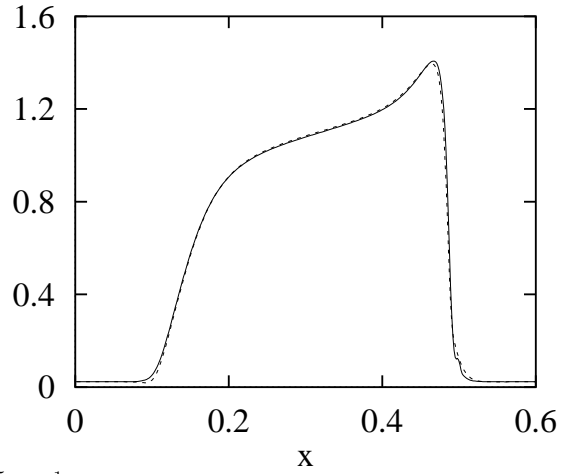
Fig. 5. Velocity u in $10^5 ms^{-1}$ obtained with Kinetic Scheme (dashed) and finite difference scheme (solid).
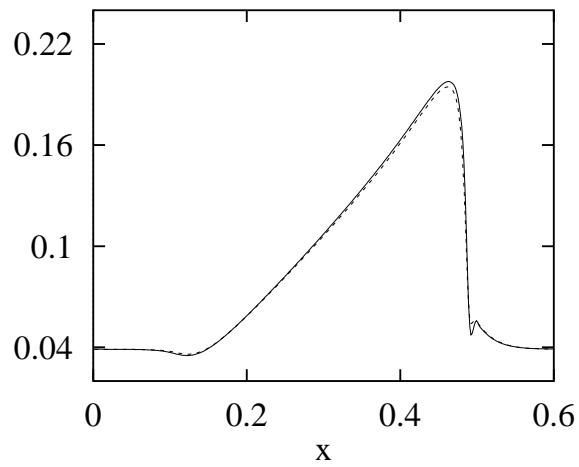

Fig. 6.   Energy W/n in eV obtained with Kinetic Scheme (dashed) and finite difference scheme (solid)

Although a possible irregularity of the solution appears near the second junction the two numerical schemes give the same results (up to deviations due to differences in the truncation error).
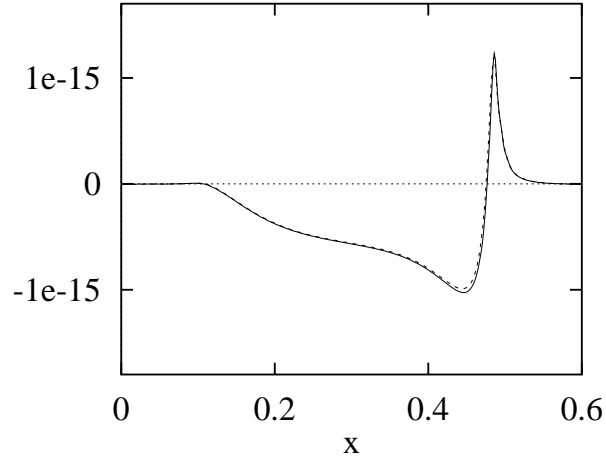

Fig. 7.   Heat flux q/n in Jms^{-1} obtained with Kinetic Scheme (dashed) and finite difference scheme (solid).
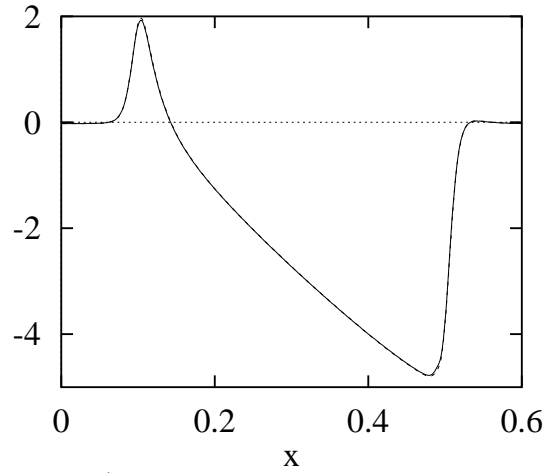
Fig. 8.   Electric field E in $kVcm^{-1}$ obtained with Kinetic Scheme (dashed) and finite difference scheme (solid).

We conclude with a remark on the hyperbolicity of the system. The normalized quantities $\hat{u}$ and $\hat{q}$ are plotted together with the hyperbolicity boundary (Fig. 9). The solution lies inside the hyperbolicity region. However, if the linear closure is used in the same setup, we see that hyperbolicity is lost in parts of the domain (Fig. 10). The difference between linear and non linear closure in the velocity curve is shown in Figure 11, and the comparison of heat fluxes is given in Fig. 12.
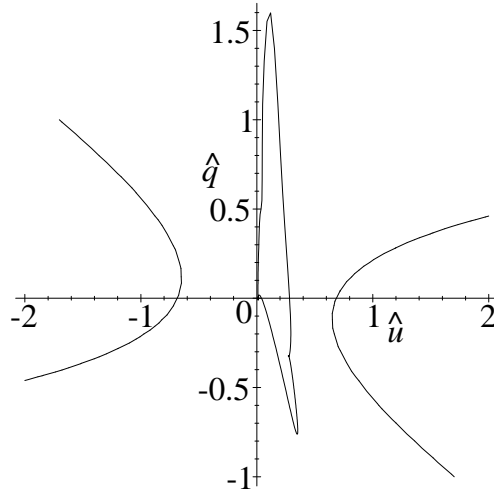
Fig. 9. Solution in the hyperbolicity region (nonlinear closure).
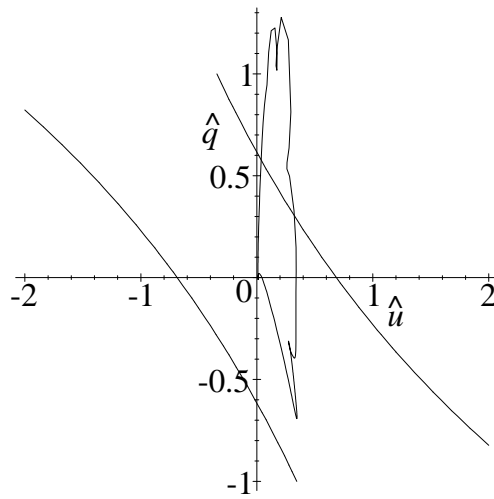

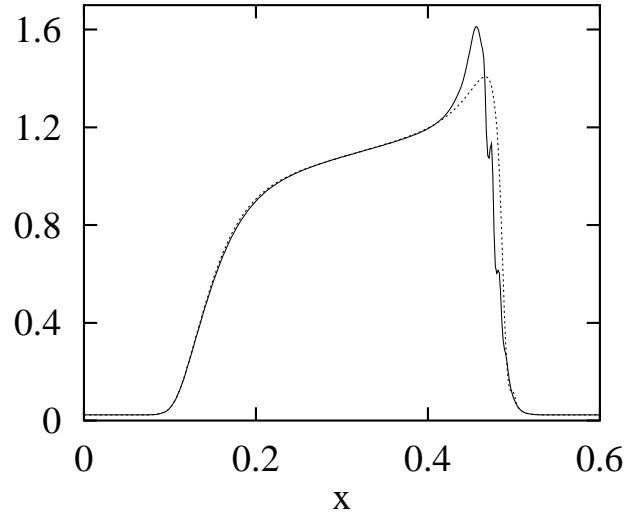Fig. 10. Solution leaving the hyperbolicity region (linear closure).

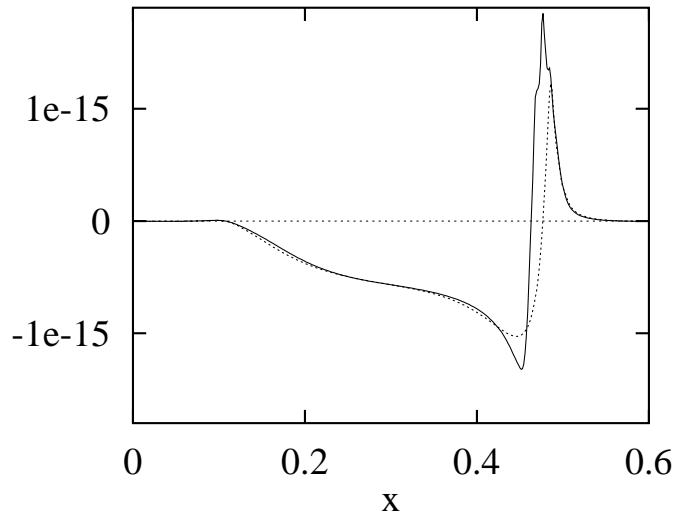Fig. 11.   Velocity distribution in linear (solid) and nonlinear closure (dotted).

Fig. 12.   Heat flux distribution in linear (solid) and nonlinear closure (dotted).

7. Conclusions

The good agreement even on non smooth solutions between the numerical results given by two methods based on completely different approaches, lends us confidence on the validity of the results of the simulations.

It also turns out, that the hydrodynamical semiconductor model based on a closure which is nonlinear in the heat flux is more suitable than the one based on a linear closure. The numerical results are more stable and the type of the equation does not change in the presence of high heat fluxes at moderate flow velocities.

Some open problems remain. They are mainly related to the singular behavior near the second junction. The main point here is the observation that two completely different methods give essentially the same numerical solution. This is an indication that the observed singularity is not a numerical artifact and can be viewed as an indication that the two methods have the same numerical entropy. However if the irregularity is a delta-shock then the meaning of the viscous solution is not clear. These topics deserve further analysis.

8. Acknowledgements

References

1. A. M. Anile and O. Muscato, *Improved hydrodynamical model for carrier transport in semiconductors*, Phys. Rev. B., **51** (1995) 16728–16740.
2. A. M. Anile and S. Pennisi, *Thermodynamic derivation of the hydrodynamical model for charge transport in semiconductors*, Phys. Rev. B, **46** (1992) 13186–13193.
3. A. M. Anile, V. Romano and G. Russo, *Hyperbolic hydrodynamical models of carrier transport in semiconductors*, VLSI Design, **8** (1998) 521–525.
4. A. M. Anile, V. Romano and G. Russo, *Extended hydrodynamical models of carrier transport in semiconductors*, preprint.
5. A. M. Anile and M. Trovato, *Nonlinear closures for hydrodynamical semiconductors transport models*, Physics Letter A, **230** (1997) 387–395.
6. J. D. Au, *Nonlinear Closure in Molecular Extended Thermodynamics with Application to the Shock Wave Structure Solution*, Supplemento ai Rendiconti del Circolo Matematico di Palermo, **45** (1996) 59–67.
7. R. E. Caflisch, G. Russo, and Shi Jin, *Uniformly Accurate Schemes for Hyperbolic Systems with Relaxation*, SIAM J. Numer. Anal., **34** (1997) 246–281.
8. C. Cercignani, **The Boltzmann Equation And Its Applications**, (Springer, 1988).
9. S. M. Deshpande, *Kinetic theory based new upwind methods for inviscid compressible flows*, AIAA paper, **86–0275** (1986) .
10. W. Dreyer, *Maximization of the entropy in non-equilibrium*, J. Phys. A:Math. Gen., **20** (1987) 6505–6517.
11. M. V. Fischetti and S. Laux, *Monte Carlo study of electron transport in silicon inversion layers*, Phys. Rev. B, **48** (1993) 2244–2274.

12. A. Harten and S. Osher, *Uniformly high-order accurate nonoscillatory schemes. I.*, *SIAM J. Numer. Anal.*, **24** (1987) 279–309.

13. A. Harten, P. D. Lax and B. van Leer, *On upstream differencing and Godunov–type schemes for hyperbolic conservation laws*, *SIAM Rev.*, **25** (1983) 35–61.

14. S. Jin, *Modern shock capturing methods for conservation laws*, in *Some New Directions in Science on Computers*, eds. G. Bahnot, S. Y. Chen, and P. Seiden, World Scientific.

15. S. Jin, and Z.P. Xin, *The relaxation schemes for systems of conservation laws in arbitrary space dimensions*, *Comm. Pure Appl. Math.*, **48** (1995) 235–276.

16. D. Jou, J. Casas-Vazquez and G. Lebon, **Extended Irreversible Thermodynamics**, (Springer-Verlag, 1993).

17. M. Junk, *Kinetic Schemes: A new approach and applications*, Ph.D. thesis, Universität Kaiserslautern.Shaker Verlag, Aachen, 1997

18. S. Kaniel, *A Kinetic Model for the Compressible Flow Equation*, *Indiana Univ. Math. J.*, **37** (1988) 537–563.

19. C. D. Levermore, *Moment Closure Hierarchies for Kinetic Theories*, *J. Stat. Phys.*, **83** (1996) 331–407.

20. F. Liotta, V. Romano and G. Russo, *Central Schemes for Systems of Balance Laws*, in *Proceedings 7th International Conference on Hyperbolic Problems, Zürich 1997*, to appear.

21. D. G. Luenberger, **Linear and Nonlinear Programming**, (Addison–Wesley, 1989).

22. A. Majorana and G. Russo, *Stationary Solutions of Hydrodynamic Models for Semiconductor Device Simulation*, *COMPEL*, **12** (1993) 81–93.

23. A. Markowich, C. A. Ringhofer and C. Schmeiser, **Semiconductor Equations**, (Springer-Verlag, 1990).

24. I. Müller and T. Ruggeri, **Extended Thermodynamics**, (Springer-Verlag, 1993).

25. O. Muscato, R. M. Pidatella and M. Fischetti, *Monte Carlo simulation and hydrodynamic simulation of a one dimensional $n^+ - n - n^+$ silicon diode*, *VLSI*, **6** (1998) 247–250.

26. H. Nessyahu and E. Tadmor, *Non-oscillatory central differencing for hyperbolic conservation laws*, *J. Comp. Phys.*, **87** (1990) 408–463.

27. E. Fatemi, J. Jerome and S. Osher, *Solution of Hydrodynamic Device Model Using High-Order Nonoscillatory Shock Capturing Algorithms*, *IEEE Transaction on Computer-Aided Design*, **10** (1991) 232–244.

28. B. Perthame, *Boltzmann type schemes for gas dynamics and the entropy property*, *SIAM J. Numer. Anal.*, **27** (1990) 1405–1421.

29. V. Romano and G. Russo, *Numerical solutions for hydrodynamical models of semiconductors*, preprint.

30. R. H. Sanders and K. H. Prendergast, *On the origin of the 3 kiloparsec arm*, *Astrophys. Journal*, **188** (1974) 489–500.

31. G. Strang, *Accurate Partial Difference Methods II: Nonlinear Problems*, *Num. Math.*, **6** (1964) 37–46.

32. D. Tan, T. Zhang and Y. Zheng, *Delta-shock waves as limits of vanishing viscosity for hyperbolic systems of conservation laws*, *J. Diff Equation*, **112** (1994) 1–32.

33. B. Van Leer, *Towards the ultimative conservative difference scheme. V: A second-order sequel to Godunov's method*, *J. Comp. Phys.*, **32** (1979) 101–136.